DEUTSCHES ELEKTRONEN-SYNCHROTRON DESY

DESY SR-84-003
February 1984

A COMPTON POLARIMETER FOR SYNCHROTRON RADIATION IN THE X-RAY ENERGY RANGE

by

F. Smend, D. Schaupp, H. Czerwinski

II. Physikalisches Institut der Universität Göttingen

A.H. Millhouse, H. Schenk-Strauss

Fachrichtung 17.3, Universität des Saarlandes

ISSN 0723-7979

NOTKESTRASSE 85 · 2 HAMBURG 52

DESY SR-84-003
February 1984

ISSN 0723-7979

A Compton Polarimeter for Synchrotron Radiation in the X-Ray Energy Range*

F. Smend, D. Schaupp, H. Czerwinski
II. Physikalisches Institut
der Universität Göttingen
A. H. Millhouse, H. Schenk-Strauss
Fachrichtung 17.3
Universität des Saarlandes

Abstract

A polarimeter for synchrotron radiation in the energy range $E \gtrsim 15$ keV is described. It utilizes 90° Compton scattering by low-Z atoms in a thin organic foil. The effect of double scattering on the analyzing power is calculated. The instrument can be used for continuously monitoring the intensity and the polarization of a photon beam during an experiment.

* Supported by Bundesministerium für Forschung und Technologie

ISSN 0723-7979

Introduction

Polarimeters for X-rays are based upon one of those photon scattering processes whose differential cross sections depend in a well-known way on the polarization of the photon beam.

In case of linear polarization, Rayleigh scattering by bound electrons[1,2] or Compton scattering by free electrons[3], each through the scattering angle $\vartheta = 90°$, may be utilized. In the X-ray region both of these processes are, to a good approximation, of dipole character. This means that, at $\vartheta = 90°$, the differential cross section is nearly proportional to $\sin^2\varphi$, where φ is the angle between the plane of polarization and the scattering plane.

Materlik and Suortti[4] utilized Rayleigh scattering by a Molybdenum target, enhanced by coherent Bragg reflexion at $\vartheta = 2\Theta_B = 90°$. Obviously, this method can be applied only at those discrete values of the photon energy, for which the Bragg condition is fulfilled with $2\Theta_B = 90°$. The integrated intensity of a Bragg peak at 90° decreases strongly with increasing photon energy. This fact limits the use of a Rayleigh-Bragg polarimeter to photon energies up to about 15 keV. Materlik and Suortti used an "infinitely thick" scattering target, which does not allow the polarimeter to be used as a polarization monitor during an experiment.

Tolkiehn and Petersen[5] utilized Rayleigh plus Compton scattering at $\vartheta = 90°$ in a gaseous Xe-N_2 mixture. The "white" beam contained photons with energies up to about 40 keV. Compton scattering by the inner electrons of a heavy atom like Xe is, possibly, modified by effects of binding in a way that the free-electron model might not be an adequate description. However, there exists no reliable theory of binding effects in Compton scattering[6].

In the present work the polarimeter utilizes Compton scattering at $\vartheta = 90°$ by a thin Kapton foil consisting of low-Z atoms only. The Klein-Nishina formula is, therefore, expected to be adequate for calculating scattering cross sections at photon energies $E \gtrsim 15$ keV. Since only few percent of the primary beam are absorbed in the scattering foil, the instrument can be used as a transmission-type polarimeter for continuously monitoring the beam polarization during an experiment.

Apparatus

Fig. 1 shows the set-up. The monochromatized beam, having the diameter 1 mm, traverses a 28 mg/cm^2 Kapton foil oriented at 45° with respect to the beam. Photons scattered through $\vartheta = (90 \pm 1.8)°$ are detected by two 1 mm thick NaI scintillation detectors mounted behind identical collimators, being perpendicular to each other and to the beam axis as well. The Kapton scatterer is mounted on a retractable frame. For technical reasons the scatterer is positioned in "reflexion" geometry for one of the detectors and in "transmission" geometry for the other one. The effect of this difference in geometry is very small. It is determined by rotating the entire polarimeter by 90° around the beam axis.

Fig. 2 shows typical pulse-height spectra of Compton scattered photons, taken at the primary energy E = 28.5 keV. The spectra were measured with a single NaI detector mounted on the polarimeter, by rotating the polarimeter into the horizontal and vertical scattering plane, respectively, and normalizing the spectra to the count rate in another detector in the direct beam.

With careful shielding of the polarimeter, the pulse-height spectra are virtually free of background. Therefore, the scattering rates can be measured using two single-channel discriminators and CAMAC scalers. In this way the polarization of the beam can be monitored continuously during an experiment. Moreover, by adding the count rates of both detectors a count rate proportional to the total intensity of the beam is obtained. In the energy range used, no X-ray fluorescence of the Kapton foil was observed. In contrast to this, a variety of organic foils showed surprisingly strong K X-ray fluorescence in the energy range between 20 and 30 keV due to small amounts of polymerizing or stabilizing additives.

Performance

As stated above, the Klein-Nishina formula for the differential cross section for Compton scattering[3] is used in evaluating the ratio Q of the numbers of incident photons having linear polarization in the horizontal, or orbit, (H) and in the vertical (V) plane, respectively.

$$Q = N_V/N_H .$$

From Q the degree P of linear polarization follows by

$$P = (1 - Q)/(1 + Q).$$

Special attention was paid to the contribution of double scattering into $\vartheta = 90°$ for primary photons polarized parallel to the scattering plane. A detailed account of the calculation is given in the Appendix. If the incoming beam were completely polarized in the horizontal plane ($P = 1$), the ratio R = (count rate for scattering in the horizontal scattering plane)/(count rate in the vertical scattering plane) would be $R = 0.0049$ and $R = 0.0084$ for the photon energies $E = 22.5$ keV and $E = 45$ keV, respectively (see Table 1). The analyzing power $A = (1 + R)/(1 - R)$ of the polarimeter for these energies is $A = 0.990$ and $A = 0.984$, respectively. As an example, the measurements shown in Fig. 2 yield the degree of linear polarization $P = 0.942 \pm 0.003$, in fair agreement with a theoretical calculation[7] based on a general knowledge of the parameters of the electron orbit in the storage ring DORIS II.

It has to be noticed that P is just an apparent degree of linear polarization. In fact, synchrotron radiation has elliptic polarization with the two axes of the ellipse being horizontal and vertical, respectively. In an actual experiment the photon beam consists of right-handed and left-handed photons having, moreover, various ratios of the semi-axes of their respective polarization ellipses. However, the resulting degree of circular polarization cannot be measured by a Compton polarimeter containing randomly oriented electrons[8]. Whether or not a separate measurement of the degree of circular polarization is necessary depends on the experiment to be done using the photon beam.

Appendix: Correction for double scattering at the minimum position of the polarimeter

At photon energies $E \lesssim 50$ keV small corrections to the analyzing power of the Compton polarimeter may be calculated using the low-energy limit of the Klein-Nishina formula, i.e., the Thomson formula[3,9]. In case of Thomson scattering of linearly polarized photons, the differential cross section depends only on the angle γ between the electric vectors $\vec{E}_0$ and $\vec{E}_1$ before and after scattering, respectively:

$$d\sigma/d\Omega = r_0^2 \cos^2\gamma ,$$

where $r_0 = 2.818 \times 10^{-13}$ cm is the classical electron radius.

The geometry of single Thomson scattering is depicted in Fig. 3 (cf. ref. 9). The primary photon (wavevector $\vec{k}_o$, with $k_o = 2\pi/\lambda_o$) propagates along $\vec{OB}$ and has its electric vector $\vec{E}_o$ along $\vec{OD}$. Let this photon be scattered first into direction $\vec{OA}$ (wavevector $\vec{k}_1$), forming the polar angle ξ with $\vec{E}_o$ and having the azimuthal angle ϱ with respect to the $\vec{OD}$ axis. The electric vector $\vec{E}_1$ is tangential to the meridian CAD and forms the angle $\gamma_1 = \pi/2 - \xi$ with $\vec{E}_o$ (see Fig. 4). The differential cross section for the first scattering into a solid angle $\sin\xi\, d\xi\, d\varrho$ is, independently of ϱ,

$$
\begin{aligned}
d^2\sigma_1 &= r_o^2 \cos^2\gamma_1 \sin\xi\, d\xi\, d\varrho \\
&= r_o^2 \sin^3\xi\, d\xi\, d\varrho.
\end{aligned}
$$

If now the photon undergoes a second scattering such that its final wavevector $\vec{k}_2$ points into the solid angle $d\Omega_2$ around $\vec{E}_o$, or $\vec{OD}$, the angle between $\vec{E}_1$ and $\vec{E}_2$ is $\gamma_2 = \xi$. Hence, the differential cross section is

$$
\begin{aligned}
d\sigma_2 &= r_o^2 \cos^2\gamma_2\, d\Omega_2 \\
&= r_o^2 \cos^2\xi\, d\Omega_2.
\end{aligned}
$$

In order to estimate the double scattering of photons into $d\Omega_2$ at 90°, both differential cross sections have to be combined and applied to the scattering foil of the polarimeter. The geometry of the foil is shown in Fig. 5. Let the first scattering take place at O within the foil, and let again the angle between $\vec{k}_1$ and $\vec{E}_o$ be ξ, and ϱ be the azimuth around the z axis. The direction ($\xi, \varrho = 0$) is

nearest to the normal on the foil. Then, the once-scattered photon would have to traverse the path $\vec{L}(\xi,\varrho)$ in the foil before emerging at surface a or b. The locus of all paths $\vec{L}(\xi,\varrho)$ is a cone around the z-axis with its top in O and with ξ being the angle of aperture (Fig. 5). The path length $L(\xi,\varrho)$ follows from a straightforward geometrical consideration. We define the quantity

$$\varphi(\xi,\varrho) = -\arctan(\tan\xi\cos\varrho)$$

which is the angle between the z axis and the projection of $\vec{L}$ on the plane containing both the z axis and the normal on the foil. φ runs from $-\xi$ at $\varrho = 0$ to ξ at $\varrho = \pi$. Then we obtain

$$L(\xi,\varrho) = \frac{\cos\varphi}{|\cos\xi|\,\sin|\alpha-\varphi|} \times \begin{cases} s & \text{(a)} \\ (t-s) & \text{(b)} \end{cases}$$

with (a) and (b) standing for emergence through surfaces a and b, respectively. The conditions for case (a) or (b) to apply, are

	$0 \le \xi \le \pi/2$	$\pi/2 < \xi \le \pi$
$-\xi \le \varphi < \mathrm{Min}(\alpha,\xi)$	(a)	(b)
$\alpha < \varphi < \xi$ (if $\alpha < \xi$)	(b)	(a)

The average path length $\bar{L}(\xi)$ is obtained via

$$\bar{L}(\xi) = (1/2\pi)\int_0^{2\pi} L(\xi,\varrho)\, d\varrho.$$

If N_o photons having the electric vector $\vec{E}_o$ in the z direction are incident on the scattering foil, the number N_2 of photons double-scattered through 90° into the solid angle $d\Omega_2$ around the z direction is given by

$$N_2 = N_o\, d\Omega_2\, n^2\, t_{eff}\, r_o^4\, 2\pi \int_0^{\pi} \bar{L}'(\xi)\, \sin^3\xi\, \cos^2\xi\, d\xi .$$

Here, n is the number density of electrons in the foil and t_{eff} the effective thickness of the foil for the incident photons. Since the detector is viewing, through its collimator, only a limited area of the scattering foil, a suitable upper limit L_{max} for $L(\xi,\varrho)$ is introduced before averaging:

$$\bar{L}'(\xi) = (1/2\pi) \int_0^{2\pi} \mathrm{Min}[L(\xi,\varrho),\, L_{max}]\, d\varrho .$$

For a scattering foil having the thickness $t = 0.02$ cm, the effective thickness $t_{eff} = 0.028$ cm, and the number density $n = 4.6 \times 10^{23}$ cm^{-3}, forming the angle $\alpha = 30°$ with the z axis, the quantity $N_2/(N_o\, d\Omega_2)$ was calculated for different values of s by numerical integration and, after that, averaged over s. L_{max} was set equal to 0.5 cm. The result of the calculation is

$$N_2/(N_o\, d\Omega_2) = 3.3 \times 10^{-6}\ sr^{-1} .$$

It may be assumed that this value, although calculated for

double scattering exactly into the z direction, may be taken as nearly constant over the small range of scattering angles accepted by the detector.

The same does not hold for the differential cross section for single Compton scattering by angles near $\vartheta = 90°$ and near the $\vec{k}_o, \vec{E}_o$ plane, i.e., $\varphi \approx 0$. According to the Klein-Nishina formula, a minimum is obtained very close to $(\vartheta = 90°,\ \varphi = 0°)$, i.e., the direction of $\vec{E}_o$. However, the cross section is rising strongly when leaving the minimum direction. By averaging over the range of scattering directions (ϑ, φ) accepted by the detector, the effective ratio $N_{\parallel}/(N_o\, d\Omega_2)$ for single Compton scattering at the minimum position of the detector was calculated for the photon energies $E = 22.5$ keV and 45 keV. The results are given in Table 1, together with $N_{\perp}/(N_o\, d\Omega_2)$, i.e., the effective ratio for single Compton scattering by $\vartheta = 90°$, $\varphi = 90°$. In addition, the intensity ratio $R = (N_{\parallel} + N_2)/N_{\perp}$ is shown, and the analyzing power A, defined by

$$A = (1 - R)/(1 + R) .$$

The degree of linear polarization is obtained from the ratio F_b/F_a of the count rates in the detectors (see Fig. 2) by the expression

$$P = (1/A)\,(1 - F_b/F_a)/(1 + F_b/F_a) .$$

References

1. Kissel,L., and Pratt,R.H.: Rayleigh Scattering: Elastic Photon Scattering by Bound Electrons. To be published in: Atomic Inner-Shell Physics (B. Crasemann, ed.)
2. Kissel,L., Pratt,R.H., and Roy,S.C., Phys. Rev. A 22, 1970 (1980)
3. Heitler,W.: The Quantum Theory of Radiation, 3rd ed., Sect. 22. Oxford: Clarendon 1954
4. Materlik,G., and Suortti,P., Journ. Applied Crystallography (in press)
5. Tolkiehn,G., and Petersen,W., Nuclear Instr. Meth. 215, 515 (1983)
6. Botto,D.J., and Pratt,R.H., Univ. of Pittsburgh Internal Report PITT-213 (1979), unpublished
7. We thank Dr. B. Schönfeld (HASYLAB) for providing the computer program for the calculation.
8. Nishina,Y., Z. Physik 52, 869 (1928)
9. Evans,R.D.: The Atomic Nucleus, Ch. 23. New York: McGraw-Hill 1955

Table 1 Calculated performance of the Compton polarimeter

$N_{\parallel}/(N_o\, d\Omega_2)$: scattering ratio for 90° Compton scattering in the plane of polarization of the primary beam;

$(N_{\parallel}+N_2)/(N_o\, d\Omega_2)$: same as before, but with the effect of double scattering added;

$N_{\perp}/(N_o\, d\Omega_2)$: scattering ratio for 90° Compton scattering perpendicular to the plane of polarization;

$R = (N_{\parallel}+N_2)/N_{\perp}$;

$A = (1-R)/(1+R)$: analyzing power of the polarimeter.

E keV	$N_{\parallel}/(N_o\, d\Omega_2)$ 10^{-6} sr^{-1}	$(N_{\parallel}+N_2)/(N_o\, d\Omega_2)$ 10^{-6} sr^{-1}	$N_{\perp}/(N_o\, d\Omega_2)$ 10^{-6} sr^{-1}	R	A
22.5	1.3	4.6	939	0.0049	0.990
45	3.5	6.8	867	0.0078	0.984

Figure captions

Fig. 1 Schematic drawing of the polarimeter. The photon beam (diameter 1 mm) is perpendicular to the plane of the drawing and crosses the Kapton foil in B. The Kapton foil (thickness 28 mg/cm^2) is tilted by 45° around the axis AC with respect to the plane of the drawing. It can be moved out of the beam into direction A. Each of the two collimators for the scattered photons consists of two diaphragms D_1 (diameter 4 mm) and D_2 (diameter 5 mm). The scattered photons are detected by 25 mm Ø x 1 mm NaI detectors. The polarimeter is part of an evacuated beam tube. It can be rotated by 90° around the beam axis.

Fig. 2 Pulse height spectra of 28.5 keV photons scattered by 90°, measured in (a) the vertical and (b) the horizontal scattering plane. Background is not subtracted. The spectra were taken behind a Ge(111) double Bragg monochromator at beam G3 of the storage ring DORIS II at the electron energy 3.5 GeV. The recording times were (a) 150 s and (b) 400 s, respectively. In the figure, spectrum (b) is normalized to the recording time of spectrum (a). The intensity ratio of the two spectra is $F_b/F_a = (3.53 \pm 0.12)\times 10^{-2}$.

Fig. 3 Geometry of Thomson scattering at O. OB: direction of primary wavevector $\vec{k}_o$; OA: direction of scattered wavevector $\vec{k}_1$; ξ, φ : polar and azimuthal angles of $\vec{k}_1$; $\vec{E}_o$, $\vec{E}_1$: electric vectors before and after scattering.

Fig. 4 The plane OCAD of Fig. 3, showing the electric vector $\vec{E}_2$ after the second scattering into the OD, or z, direction.

Fig. 5 Geometry of the scattering foil in the polarimeter. α is the angle between the foil and the z axis, which points to the detector. t is the foil thickness, and s the depth of the point O of first scattering below surface a of the foil. The incident photon beam lies in the plane perpendicular to z with its electric vector $\vec{E}_o$ parallel to z.

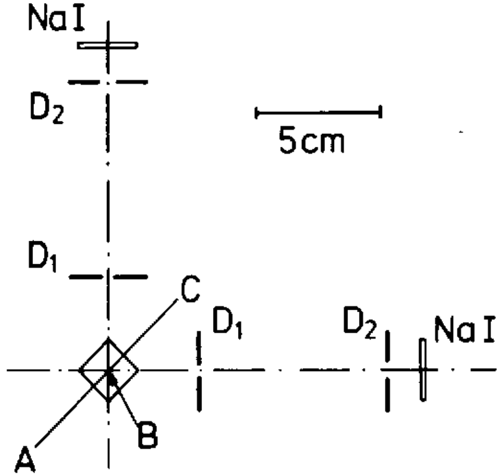
NaI
D2
5cm
D1
C
D1
D2
NaI
B
A

Fig. 1

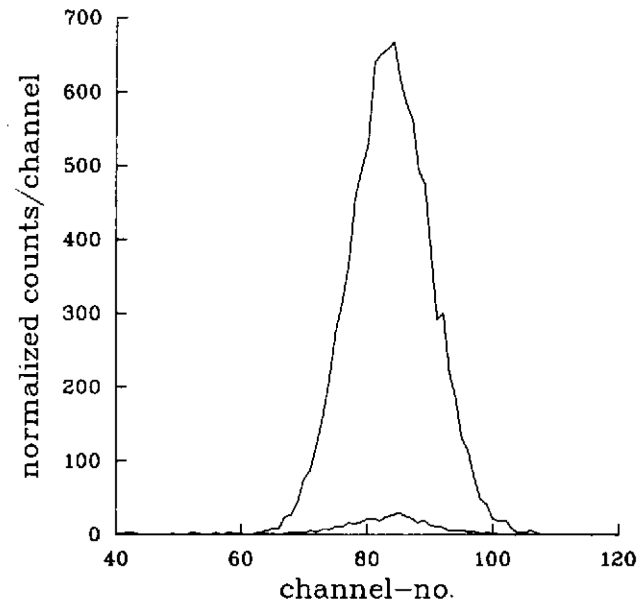
700
600
500
400
300
200
100
0
normalized counts/channel
40
60
80
100
120
channel-no.

Fig. 2

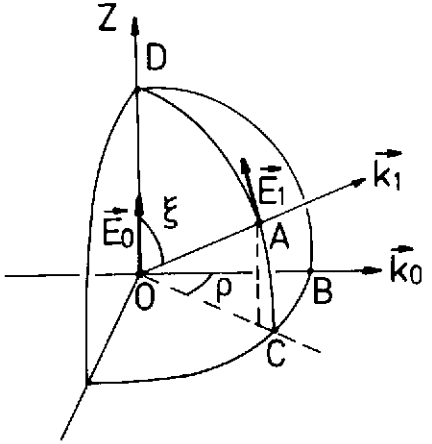
Z
D
$\vec{E}_1$
$\vec{k}_1$
$\vec{E}_0$
ξ
A
$\vec{k}_0$
O
ρ
B
C

Fig. 3

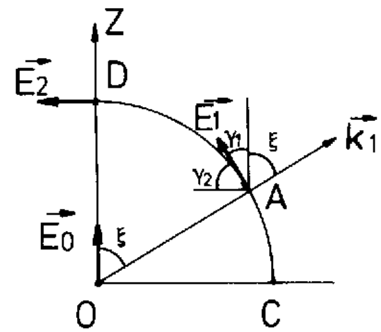
Z
$\vec{E}_2$
D
$\vec{E}_1$
γ_1
ξ
$\vec{k}_1$
γ_2
A
$\vec{E}_0$
ξ
O
C

Fig. 4

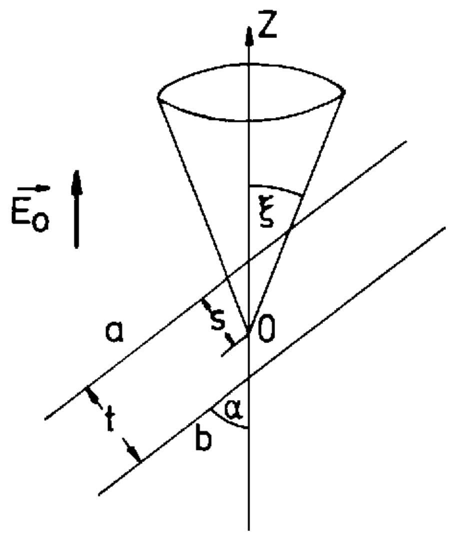

Fig. 5